Science Translational Medicine
AAAS

www.sciencetranslationalmedicine.org/cgi/content/full/10/443/eaap8373/DC1

Supplementary Materials for

Proprioception from a neurally controlled lower-extremity prosthesis

Tyler R. Clites, Matthew J. Carty, Jessica B. Ullauri, Matthew E. Carney,
Luke M. Mooney, Jean-François Duval, Shriya S. Srinivasan, Hugh. M. Herr*

*Corresponding author. Email: hherr@media.mit.edu

Published 30 May 2018, *Sci. Transl. Med.* **10**, eaap8373 (2018)
DOI: 10.1126/scitranslmed.aap8373

The PDF file includes:

Other Supplementary Material for this manuscript includes the following:
(available at
www.sciencetranslationalmedicine.org/cgi/content/full/10/443/eaap8373/DC1)

Materials and Methods

Subject selection (Group T)

All subjects in Group T were active and ambulatory (lower-extremity prosthesis functional level K3 or K4). Indications for these patients' amputations include one crush injury, one blast injury, one traumatic fall, and one case of hemophilic arthropathy (this patient's hemophilia is currently well managed, and he maintains an active ambulatory lifestyle). All amputation procedures were performed at various hospital sites according to the clinical standard-of-care. All subjects underwent standard-of-care rehabilitation protocols, and none of them have nerve or muscle damage within their residual limb beyond what is typical of amputation. Prior to beginning experiments, all subjects in Group T were guided through the same joint motion visualization exercises as Subject A.

Surface electrode placement and EMG processing

Electrode placement sites were identified (M.J.C.), and electrodes were placed acutely at the start of each experimental session. During electrode placement, each subject was instructed to volitionally move the phantom foot through each of the four ankle and subtalar motions, as the residuum was palpated. Placement of each electrode pair was independently validated by real-time visual inspection of the raw differential EMG signal. Insulated, passive extension cables allowed temporary surface electrodes (Coviden, Inc.) to be used inside of the socket. Raw EMG was differentially pre-amplified (20x gain), low pass filtered (1 kHz), and amplified to a range of $\pm$5 V (adjustable gain, MA300, Motion Lab Systems). This raw signal was then baseline offset and scaled to a range of 0-3 V, and sent to the analog inputs of the prosthetic embedded systems. On the prosthesis, each analog input signal was offset corrected, full-wave rectified, and integrated using a 100 ms moving average window. Amplitude of this integrated signal was calibrated to maximum voluntary contraction, and treated as a measure of activation within the associated muscle, referred to herein simply as EMG.

Controller tuning

Controller gains were tuned independently for each subject at the start of each trial day. After electrodes were placed and the system was properly calibrated, gain tuning began with adjustment of the activation threshold for each virtual muscle. Next, we tuned the relative torque-producing capacity of each virtual muscle, which affected prosthetic responsiveness. Once each virtual muscle had been tuned, we adjusted the minimum co-activation required for increasing joint impedance. It is noteworthy that this threshold required substantial modification in Subjects T2 and T4, to account for inadvertent co-contraction. All values were tuned until the subject felt that modifications would no longer improve performance. After tuning was complete, subjects were allowed time for exploratory control of the prosthesis (30-60 mins, depending on subject preference) before beginning experiments.

Fine-wire electrode placement and stimulation

During placement of fine-wire electrodes, Subject A volitionally moved the phantom foot through each of the four ankle and subtalar motions while the residuum was palpated to identify the four AMI muscles. Fine-wire intramuscular electrodes (Motion Lab Systems) were then inserted (M.J.C) into each muscle of interest. Placement was verified electromyographically and via direct muscle stimulation, as described below. Muscle contraction was observable both visually and through palpation. Poorly-placed electrodes were removed and replaced. To account for changes in stimulation threshold associated with electrode placement, each experiment involving stimulation was carried out in its entirety in a single day, without electrode replacement. For all trials, the muscle was stimulated with a 50 Hz, current-controlled, charge-balanced, asymmetric, biphasic pulse train (NL800, Digitimer). This stimulation frequency was selected to ensure fused tetanus at all relevant stimulus amplitudes, thereby simplifying the stimulus control algorithm to require modulation only of a single

parameter. At the low stimulus amplitudes used in the study, and with the substantial rest allowed between relatively short stimulus pulse trains, the stimulated muscles did not appear to fatigue during experiments. The subject did not report any symptoms of muscle fatigue, and no decrease in performance or perception was observed over time. The pulse width of the cathodic phase was 200 μs and that of the anodic phase was 400 μs. For the closed-loop torque control experiments, the cathodic current amplitude was modulated in linear proportionality to prosthetic torque (measured or simulated), and ranged from 0 – 9 mA.

Placement was performed by an experienced clinician (M.J.C) according to the following procedure:

1. Identify target muscle pairs via palpation during volitional activation. Mark target insertion points with a marker.
2. Connect an external ground reference electrode to the patella.
3. Clean and sterilize the insertion area.
4. Open and inspect the sterile electrodes to ensure presence of two bared leads, and absence of any kinks or breakages.
5. Insert the needle smoothly to the desired starting depth (approximately 5 mm).
6. Connect EMG pre-amplifier screw terminals to electrode leads.
7. Instruct the patient to move the phantom ankle in the direction associated with contraction of the desired muscle.
8. Note the amplitude of the EMG signal envelope.
9. Advance the needle slowly until a sharp increase in EMG activity is observed. Make note of the estimated needle depth and amplitude of signal envelope.
10. Carefully withdraw the needle, leaving the fine-wire pair in place within the muscle. Secure the leads to the skin with tape at the insertion point and further up the leg.
11. Confirm electrode placement via palpation and visual observation of muscle contraction during 2-3 mA stimulation.

This placement protocol was modeled after the technique used clinically for needle-based EMG acquisition. In the clinic, ultrasound guidance is also sometimes used to ensure proper placement; given the easily identifiable, isolated, and superficial positioning of the target tibialis anterior muscle, this was deemed unnecessary for our purposes.

After each time an electrode was inserted, correct placement was confirmed via palpation and visual observation of the muscle during delivery of a 2 or 3 mA stimulus pulse train. In cases where the electrode was placed correctly, muscle contraction was clearly identifiable. Because the tibialis anterior is large and positioned superficially, muscle contraction could be observed via conspicuous bulging beneath the skin (movie S5). Muscle contraction was further confirmed by the clinician via palpation. When the electrode was not placed correctly within the muscle, contraction was not observed, indicating that the electrode was likely embedded in the cutaneous tissue surrounding the muscle. In these cases, the patient reported either no sensation, or a faint tingling/burning at the electrode site.

Further confirmation of correct placement was conducted via analysis of EMG during volitional motion of the phantom limb. A representative plot of those EMG data, as recorded from the *tibialis anterior*, is shown in fig. S2. The recorded electrical signal has the morphology and magnitude of raw intramuscular EMG (on the order of mV), and was also only observed during dorsiflexion (DF) of the

phantom ankle, and not plantarflexion (PF), inversion (IN), or eversion (EV), indicating successful placement of the electrodes in the tibialis anterior.

Once electrode placement was confirmed, we were purposeful in our decision to conduct the described studies in the minimum-viable amplitude range, to avoid fatigue and muscle tissue damage. We selected a 0-4 mA stimulation range for the psychometric tests and a 0-9 mA stimulation range for the torque feedback system.

Ultrasound image processing

Ultrasound images were captured on a portable high-definition ultrasound scanner at 30 fps (LS128, Telemed). Fascicle tracking was performed using the UltraTrack software (version 4) as described in *(72)*. Each muscle fascicle was identified as a segment between the parallel deep and superficial fascial lines in muscle tissue. The UltraTrack software calculated changes in length over the course of the ultrasound video using a Lucas–Kanade optical flow algorithm. Fascicle strain was then derived as fascicle length minus baseline fascicle length, divided by baseline fascicle length. Any baseline shift over the course of a trial was manually corrected by superimposing a linear slope across known regions of zero strain. EMG for these ultrasound trials was collected at 2 kHz (Trigno, Delsys Inc.). In post-processing, the EMG data were high pass filtered at 70 Hz, full-wave rectified, and integrated using a 100 ms moving average window.

Prosthetic hardware design

The two degree-of-freedom ankle-foot prosthesis was custom-developed for this study by several of the co-authors. The device is actuated by symmetrically configured brushless outrunner motors (U8, Tmotor), attached to dual stage timing-belt pulley reductions, which independently transmit torque through a four-bar linkage to a spherical, differential output. When the motors act synchronously, subtalar joint inverts and everts. The overall transmission ratio of the ankle varies circumferentially from 35:1 towards a torque singularity at the extremes of the linkage arm plantar and dorsiflexion. The functional range of motion of the ankle is approximately 25 degrees, with 10 degrees allocated to dorsiflexion and 15 degrees allocated to plantar flexion. The subtalar range of motion is approximately 30 degrees, allocated evenly to inversion and inversion.

The prosthesis uses the FLEXible, Scalable Electronics Architecture (FlexSEA) embedded system, an accessible open-source hardware and software toolkit optimized for wearable robotics applications *(73)*. One FlexSEA-Execute advanced motion controller *(74)* is used to control each motor. The Execute board is responsible for low-level control loops, and utilizes a field-oriented control (FOC) strategy to efficiently drive the brushless motor. One FlexSEA-Manage *(73)* hosts the high-level controller. This board reads EMG signals as analog inputs (4 channels), and sends motor current commands to the two FlexSEA-Execute circuits via RS-485. A PC-hosted custom user interface (LabVIEW), connected to FlexSEA-Manage via USB, allows data logging and visualization, as well as manipulation of experimental parameters.

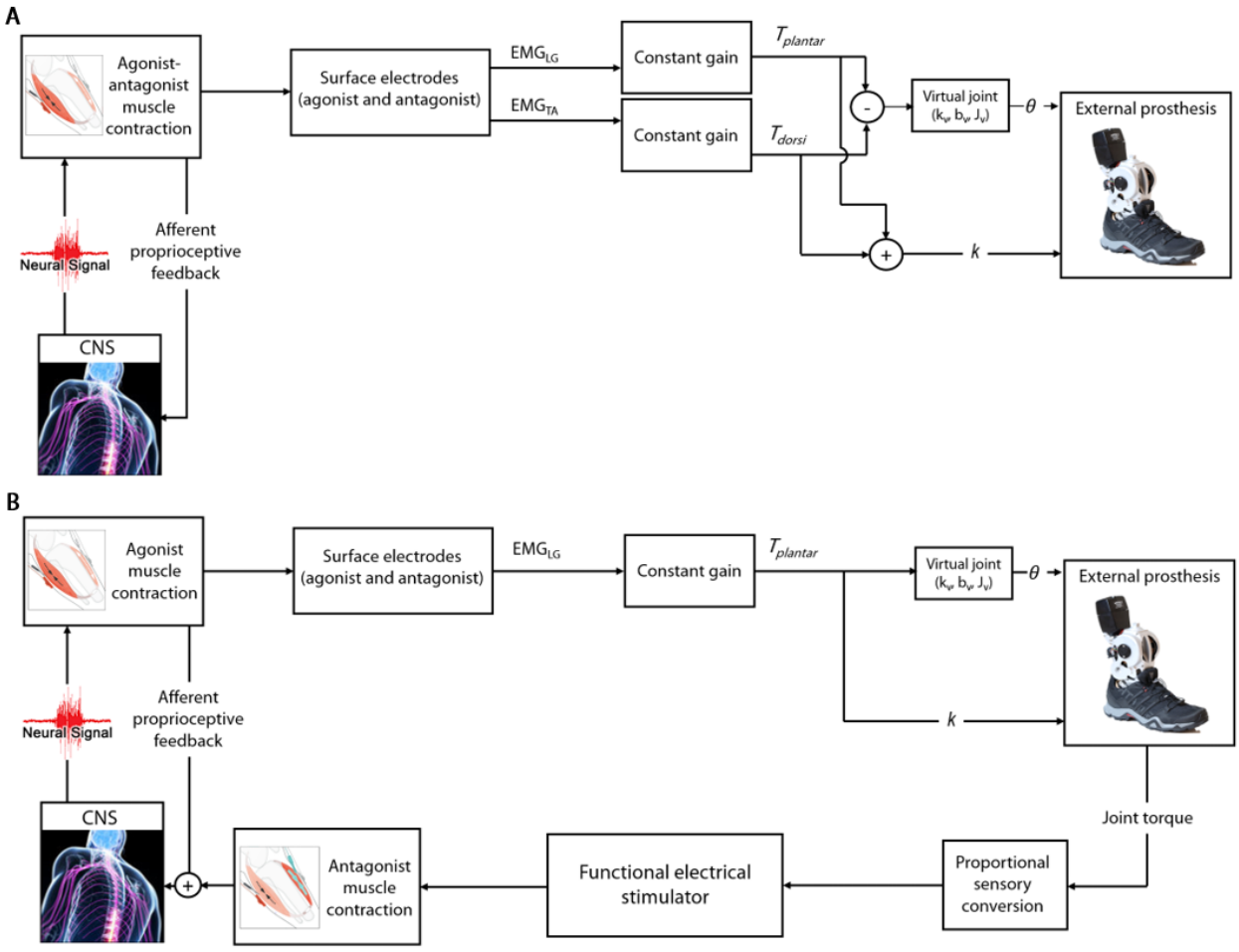

Fig. S1. Control diagrams showing how EMG from the AMI muscles drives movement of the prosthetic joint. (**A**) The prosthesis-not-in-the-loop control architecture is built around a virtual joint with physiological values of stiffness (k_v), damping (b_v), and inertia (J_v). Prosthetic joint angle (θ) is modulated by the arithmetic difference between empirically-estimated torque contributions from the AMI agonist and antagonist muscles. Joint stiffness (k) is modulated by the arithmetic sum of these torque contributions. Afferent feedback describing muscle activation is communicated by the AMI to central nervous system (CNS). Although only the ankle joint is represented here, comprised of the *lateral gastrocnemius* (LG) and *tibialis anterior* (TA), the control strategy for the subtalar joint is identical. (**B**) In the prosthesis-in-the-loop control architecture, during muscle stimulation for prosthesis joint torque feedback, the stimulated muscle is ignored (assumed to have zero activation). This limits the effect of stimulation noise on system performance.

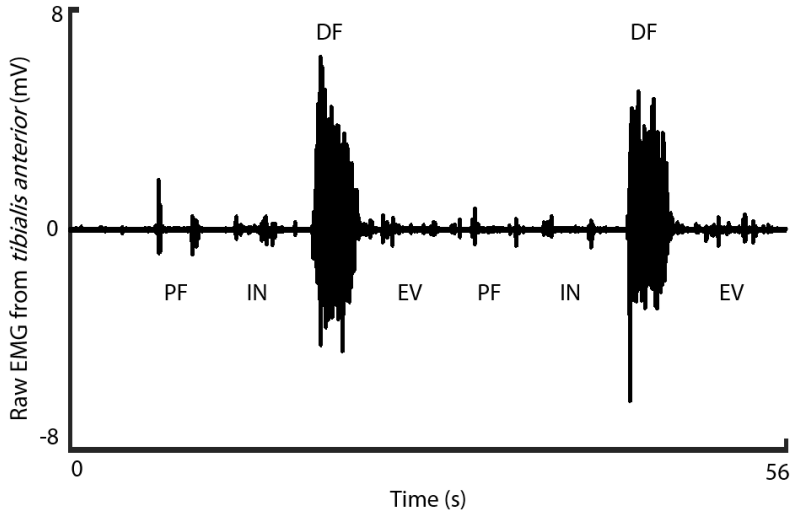

Fig. S2. Raw EMG recorded from fine-wire electrodes during volitional movement of the phantom limb. Representative trace (n = 3) of raw EMG recorded from fine-wire electrodes placed in the tibialis anterior of Subject A, during volitional plantar flexion (PF), inversion (IN), dorsiflexion (DF), and eversion (EV) of his phantom ankle and subtalar joints.

Movie S1. Ultrasound video of coupled AMI motion. In the first segment, stretch is shown in the *peroneus longus* of Subject A during volitional inversion of his phantom subtalar. In the second segment, alternating stretch and contraction are shown in the *tibialis anterior* during cyclic plantar and dorsiflexion of his phantom ankle. In the third segment, sliding of the synovial canal is visible during cyclic inversion and eversion of his phantom subtalar.

Movie S2. Volitional control. In the first segment, Subject A demonstrates his volitional control over movement of the prosthesis in the four cardinal directions of the ankle and subtalar joints. His intact limb is mirroring the intended movement of his phantom. Subject T2 is then shown performing the same task. Movement of the prosthesis appears rough and unstable. The second segment shows Subject A volitionally everting the prosthetic subtalar to prepare for foot placement on an obstacle in his path. Subject T2 is then shown performing the same task, with visible instability in the prosthetic subtalar.

Movie S3. Reflexive control. In the first segment, Subject A reflexively plantar flexes the prosthetic ankle while descending stairs. Subject T2 is then shown performing the same task, with no visible movement of the prosthetic subtalar. The second segment shows Subject A reflexive dorsiflex the prosthetic ankle while ascending stairs. Subject T4 is then shown performing the same task, with no visible dorsiflexion of the prosthetic ankle, and instability in the prosthetic ankle and subtalar joints. In the third segment, Subject A ascends stairs backwards, while explaining that he is not thinking about the observed plantar flexion. Subject T2 is then shown performing the same task, with no visible plantar flexion.

Movie S4. Candid videos showing prosthesis embodiment. In the first segment, Subject A reacts naturally to a roll of tape stuck to his shoe. In the second segment, Subject A fidgets with his prosthetic foot while having a conversation.

Movie S5. Visual confirmation of stimulated muscle contraction. Subject A's *tibialis anterior* is shown contracting under artificial stimulus via fine wire electrodes, indicating that the stimulation settings were sufficient to induce muscle contraction.